Received: 10 November 2022 | Revised: 30 April 2023 | Accepted: 10 May 2023

DOI: 10.1002/jnr.25205

RESEARCH ARTICLE

Journal of Neuroscience Research

Deciphering the causal relationship between blood pressure and regional white matter integrity: A two-sample Mendelian randomization study

Zhenyao Ye[1,2] | Chen Mo[3] | Song Liu[4] | Si Gao[1] | Li Feng[5] | Boao Zhao[6] | Travis Canida[7] | Yu-Chia Wu[6] | Kathryn S. Hatch[1] | Yizhou Ma[1] | Braxton D. Mitchell[8] | L. Elliot Hong[1] | Peter Kochunov[1] | Chixiang Chen[2] | Bingxin Zhao[9] | Shuo Chen[1,2] | Tianzhou Ma[6]

[1]Maryland Psychiatric Research Center, Department of Psychiatry, School of Medicine, University of Maryland, Baltimore, Maryland, USA

[2]Division of Biostatistics and Bioinformatics, Department of Epidemiology and Public Health, School of Medicine, University of Maryland, Baltimore, Maryland, USA

[3]Beth Israel Deaconess Medical Center, Harvard Medical School, Boston, Massachusetts, USA

[4]School of Computer Science and Technology, Qilu University of Technology (Shandong Academy of Sciences), Jinan, China

[5]Department of Nutrition and Food Science, College of Agriculture & Natural Resources, University of Maryland, College Park, Maryland, USA

[6]Department of Epidemiology and Biostatistics, School of Public Health, University of Maryland, College Park, Maryland, USA

[7]Department of Mathematics, The College of Computer, Mathematical, and Natural Sciences, University of Maryland, College Park, Maryland, USA

[8]Department of Medicine, University of Maryland School of Medicine, Baltimore, Maryland, USA

[9]Department of Statistics, Purdue University, West Lafayette, Indiana, USA

Correspondence
Tianzhou Ma, Department of Epidemiology and Biostatistics, School of Public Health, University of Maryland, College Park, MD, USA.
Email: tma0929@umd.edu

Shuo Chen, Maryland Psychiatric Research Center, Department of Psychiatry, School of Medicine, University of Maryland, Baltimore, MD, USA.
Email: shuochen@som.umaryland.edu

Funding information
National Institute on Drug Abuse (NIDA) of National Institutes of Health; National Institutes of Health, Grant/Award

Abstract

Elevated arterial blood pressure (BP) is a common risk factor for cerebrovascular and cardiovascular diseases, but no causal relationship has been established between BP and cerebral white matter (WM) integrity. In this study, we performed a two-sample Mendelian randomization (MR) analysis with individual-level data by defining two nonoverlapping sets of European ancestry individuals (genetics–exposure set: $N = 203{,}111$; mean age = 56.71 years, genetics–outcome set: $N = 16{,}156$; mean age = 54.61 years) from UK Biobank to evaluate the causal effects of BP on regional WM integrity, measured by fractional anisotropy of diffusion tensor imaging. Two BP traits: systolic and diastolic blood pressure were used as exposures. Genetic variant

Abbreviations: BP, blood pressure; BMI, body mass index; CVD, cerebrovascular and cardiovascular disease; CI, confidence interval; DTI, diffusion tensor imaging; DBP, diastolic blood pressure; ENIGMA, Enhancing Neuro Imaging Genetics through Meta Analysis; FA, fractional anisotropy; FDR, false discovery rate; GWAS, genome-wide association study; GEset, genetic–exposure association set; GOset, genetic–outcome association set; gFA, general factor of fractional anisotropy; gen-IVW, generalized version of inverse-variance weights; GENO, genotype rate; HWE, Hardy–Weinberg equilibrium; ICBP, International Consortium of Blood Pressure; IV, instrumental variable; INFO, imputation quality score; InSIDE, Instrument Strength Independent of Direct Effect; LD, linkage equilibrium; LOOA, leave-one-out approach; MR, Mendelian randomization; MAF, minor allele frequency; MIND, missingness per individual; PC, principal component; QTL, quantitative trait locus; SBP, systolic blood pressure; TBSS, tract-based spatial statistics; UKB, UK Biobank; UKBL chip, UK BiLEVE Axiom arrays; UK Biobank Axiom® arrays, UKB chip; WM, white matter; WMHs, white matter hyperintensities.

Zhenyao Ye, Chen Mo, Shuo Chen, and Tianzhou Ma contributed equally to this study.

Edited by Cristina Antonella Ghiani and Elizabeth Johnson.

Number: 1DP1DA048968-01; University of Maryland; University of Maryland Grand Challenge grant, Grant/Award Number: R01MH123163, R01EB015611 and S10OD023696

was carefully selected as instrumental variable (IV) under the MR analysis assumptions. We existing large-scale genome-wide association study summary data for validation. The main method used was a generalized version of inverse-variance weight method while other MR methods were also applied for consistent findings. Two additional MR analyses were performed to exclude the possibility of reverse causality. We found significantly negative causal effects (FDR-adjusted $p < .05$; every 10 mmHg increase in BP leads to a decrease in FA value by .4% ~ 2%) of BP traits on a union set of 17 WM tracts, including brain regions related to cognitive function and memory. Our study extended the previous findings of association to causation for regional WM integrity, providing insights into the pathological processes of elevated BP that might chronically alter the brain microstructure in different regions.

KEYWORDS
blood pressure, diffusion tensor imaging, genome-wide association study, Mendelian randomization, white matter

1 | INTRODUCTION

Elevated blood pressure (BP) which will progressively develop into hypertension is among the major modifiable risk factors for cerebrovascular and cardiovascular disease (CVD) (Chobanian et al., 2003; Fuchs & Whelton, 2020). Studies have shown that high BP is associated with significant brain structure alterations, particularly in multiple frontal, striatal, and temporal regions (Gons et al., 2010). The cerebral white matter (WM) is considered critical for connecting local and distance brain regions for efficient cognitive functioning (Madden et al., 2009). Previous studies on both young and old adults have shown that strong associations between BP and WM are particularly compelling, often by measuring the fractional anisotropy (FA) of water diffusion through diffusion tensor imaging (DTI) (Maillard et al., 2012; Salat et al., 2012). Despite their strong associations, the causal directions between BP and WM integrity have not been fully established (Williamson et al., 2018). It is commonly assumed that high BP impacts WM decline (Allen et al., 2016; Taylor-Bateman et al., 2022), but there is also the possibility that impaired WM connectivity may affect central regulations of BP. Recent studies have documented the causal effect of high BP on white matter hyperintensities (WMHs) (Georgakis et al., 2020; Sargurupremraj et al., 2020) as well as WM measures that average over the whole brain (Taylor-Bateman et al., 2022). However, they tend to ignore the heterogeneous effects on different brain regions with specialized functions. Establishing the causality link between BP and regional WM is critical for identifying effective preventative approaches to reduce the clinical impact of hypertension on specific parts of the brain.

Imaging genetics is an emerging field that performs integrative analyses of imaging and omics data to gain more insights into the mechanism of disease. Large-scale consortiums, such as UK Biobank (UKB) (Sudlow et al., 2015) and Enhancing Neuro Imaging Genetics through Meta Analysis (ENIGMA) (Thompson et al., 2014), have been conducted to collect comprehensive genetic and neuroimaging data from a very large population. In this study, we used genetic, regional neuroimaging features as well as BP from the UKB cohort to investigate the causal relationship between BP and regional WM integrity by performing a two-sample Mendelian randomization (MR) analysis. Traditional observational studies only assess associations between exposure and outcome variables. Causal interpretation of observed associations must account for both confounding and reverse causality as well as other biases (Tilaki, 2012). Making use of nature's random assortment of genetic makeup, the MR methods treat genetic variant as instrumental variable (IV) to minimize the effect of confounding and evaluate the causal effect of a modifiable exposure on outcome in observational studies (Lawlor et al., 2008). The selection of genetic variants as valid IVs that satisfy the IV assumptions is central to the MR analysis. The genetic determinants of BP as well as brain WM microstructure are increasingly characterized in the literature (Evangelou et al., 2018; Sargurupremraj et al., 2020; Zhao

Significance

Causality between blood pressure (BP) and cerebral white matter (WM) integrity has not been fully established. BP has possibly heterogeneous effects on different brain regions with specialized functions. A generalized inverse-variance weighted method and other MR methods were used to evaluate the causal effects of BP on regional WM integrity measured by the fractional anisotropy of diffusion tensor imaging. Elevated BP was found to lead to the decline in WM integrity in 17 different brain regions, related to cognitive function and memory.

et al., 2021), which made it possible to identify better instruments for MR study to investigate their causal relationships.

In this study, we hypothesized that increase in BP caused decline of WM integrity in different brain regions. We considered two BP traits: systolic blood pressure (SBP) and diastolic blood pressure (DBP), and performed a two-sample MR analysis to evaluate their causal effects on 39 WM tracts measured by FA that described WM microstructures in different brain regions. We strictly followed the MR analysis assumptions to select the genetic variants as valid IVs and implemented a generalized version of inverse-variance weights (gen-IVW) MR method using data from the UKB cohort. Additionally, we also used existing large-scale meta-analyzed genome-wide association study (GWAS) summary statistics of BP to select IVs and perform MR analysis to validate our finding. Our MR results showed consistently negative causal effects of BP traits on a union set of 17 WM tracts. Among them, elevation in both SBP and DBP had the strongest adverse impacts on bilateral posterior thalamic radiation (PTR) and subfornical organ (SFO) regions, related to cognitive function and memory (Li et al., 2022; Walsh et al., 2011). We further performed two additional MR analyses by treating FA as the exposure and ruled out the possibility of reverse causality. These findings extended previous findings (Georgakis et al., 2020; Sargurupremraj et al., 2020; Taylor-Bateman et al., 2022) to provide insights into the pathological processes related to elevated BP that chronically alter the WM microstructure in different brain regions, which in turn affects the cognitive functioning.

2 | MATERIALS AND METHODS

2.1 | UK Biobank cohort and variables

The UKB is a large prospective study that recruited ~500,000 participants between 40 and 69 years at baseline from 2006 to 2010 in 22 assessment centers throughout the United Kingdom and collected comprehensive genetic and phenotypic details (Sudlow et al., 2015). It has continued to collect more data such as imaging-derived phenotypes starting from 2014 and repeat assessment data between 2012 and 2013 (Conroy et al., 2019). Since the repeat assessment data were drawn from ~20,000 participants only with a low overall response rate (~21%) (Biobank, 2013, 2014), our analyses were restricted to family-unrelated individuals of European ancestry (i.e., primarily British, Irish) and utilized data from all sites and the initial (2006–2010) and imaging (2014+) assessment visits of the UKB.

Figure 1 shows the number of subjects included at each step of the analysis. The UKB data are split into genetic/outcome and genetic/exposure data and each carefully processed with inclusion and exclusion criteria (see details in subsequent subsections). The two-sample MR analysis in UKB cohort (1) was performed on two non-overlapping sets: the set for exploring genetic–exposure association (denoted GEset) that includes genotype and BP data but no regional WM FA data; and the set for exploring the genetic–outcome association (denoted GOset) that includes genotype, BP, and regional WM FA data. We also use large-scale meta-analyzed GWAS summary statistics of BP to select IVs and combine with the GOset to perform another two-sample MR analysis (2) to validate our findings, details of this cohort can be found in Section 2.2.

2.1.1 | Genotype data

In the UKB cohort, the genotyping was conducted using both Affymetrix UK BiLEVE Axiom (denoted UKBL chip) and UK Biobank Axiom® arrays (denoted UKB chip) to capture over 90 million single nucleotide variants (SNVs) of ~500,000 subjects (Bycroft et al., 2017). We applied quality control for genotypic data by using PLINK (version 1.9, http://www.cog-genomics.org/plink/1.9/) (Chang et al., 2015) (see detailed QC procedures in Supplementary Material).

2.1.2 | Blood pressure traits

As the exposures of interest, we analyzed the following two BP traits in nonpregnant individuals with complete data collected from the initial (2006–2010) assessment visit. For each trait, two sets of measurements were taken within a 1-min interval and automated reading from Omron device (0–255) as described in the UKB protocol (https://biobank.ctsu.ox.ac.uk/crystal/crystal/docs/Bloodpressure.pdf). We then further calculated the mean of two measurements for each BP trait:

1. Systolic blood pressure (SBP). The SBP was calculated as the mean of two non-null BP measurements using phenotype codes 4080 (Systolic blood pressure, automated reading) in the UKB.
2. Diastolic blood pressure (DBP). The DBP was calculated as the mean of two non-null BP measurements using phenotype codes 4079 (Diastolic blood pressure, automated reading) in the UKB.

We excluded individuals with discordance between self-reported sex and genotype-inferred sex from genomic data. Furthermore, we excluded individuals who took antihypertensive treatments at baseline using phenotype code 20003 (Treatment/medication code) because their observed BP did not reflect the genetically predicted BP (Malik et al., 2021). We also performed the same MR analysis when we included individuals having taken antihypertensive treatments as a sensitivity analysis (Table S8).

2.1.3 | White matter integrity data

As our primary outcome, we analyzed regional WM integrity measured by FA. FA measure is a scalar value ranging from 0 to 1, which describes the degree of anisotropy of a diffusion process (Timpe et al., 2011). A greater FA value indicates that the corresponding localized WM fiber bundles are more intact reflected by higher probability

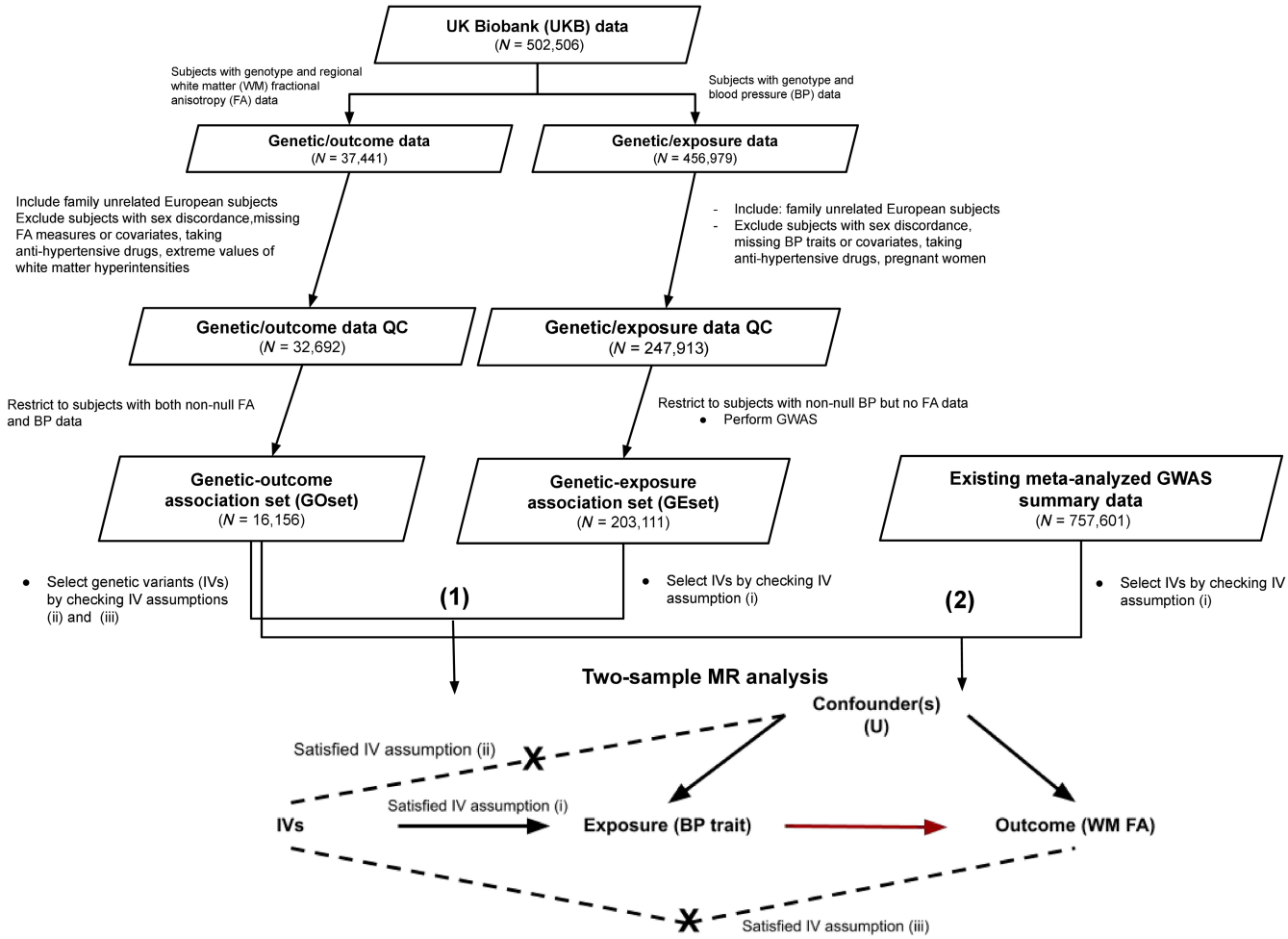

FIGURE 1 Flow chart showing the number of subjects included at each step of the analysis. On the left, the UKB data are split into genetic/outcome and genetic/exposure data and each carefully processed with inclusion and exclusion criteria. After QC step, we performed two-sample MR analysis (1) on two nonoverlapping sets: the set for exploring genetic–exposure association (denoted GEset) that includes genotype and BP data but no regional WM FA data; and the set for exploring the genetic–outcome association (denoted GOset) that includes genotype, BP, and regional WM FA data. We also used existing large-scale meta-analyzed GWAS summary statistics of BP to select IVs and combine with the GOset to perform another two-sample MR analysis (2) to validate our finding. Shown in the conceptual diagram of two-sample MR analysis, the genetic variants serve as the instrumental variables (IVs), U represents the confounder(s), BP trait is the exposure of interest and FA is the outcome in our study. The solid lines with arrows indicated the causal relationship in directed acyclic graph. Under this two-sample MR model, we aimed to assess the hypothesized causal effects of BP on regional WM FA (arrow highlighted in red). The dashed line marked with a "cross" indicates that the valid IV must be satisfied with the IV assumptions (ii) IVs should be independent of the confounders and (iii) IVs should be independent of the outcome given the exposure.

of water diffusion along the longitudinal axis of WM bundles (Timpe et al., 2011). The UKB consists of multi-modal braining imaging data covering structural, functional, and diffusion imaging based on acquisition protocol described elsewhere (Alfaro-Almagro et al., 2018). Particularly, they averaged the skeletalized images across a set of 48 standard-space tract masks according to the ENIGMA protocol for the DTI FA images to dispose of the FA images into a standard-space white matter skeleton using a tract-based spatial statistics (TBSS) analysis (Smith et al., 2006). In this study, we concentrated on a total of 39 FA tracts for multiple brain WM regions in individuals with complete data recruited in UKB at the imaging (2014+) assessment visit (see the full list of names of 39 regional WM FA tracts and their abbreviations in Table S1). We excluded individuals having extreme values of total volume of WMH using phenotype code 25781 (Total volume of white matter hyperintensities (from T1 and T2_FLAIR images) to minimize the bias (Figure S2, see more details in the Supplementary Methods) (Jones et al., 1999)).

2.1.4 | Potential confounders

The potential confounders used in our two-sample MR study as recommended by previous study (Pazoki et al., 2018) include: sex, age, body mass index (BMI), alcohol consumption and smoking status, fruit and vegetable consumption, and sedentary lifestyle (see details on their UKB phenotype codes in the Supplementary Methods). We

restricted our two-sample MR analysis to individuals with no missing values in the aforementioned set of confounders (i.e., complete case analysis) and we performed two-sample *t*-test for each confounder separately comparing the FA values of those with versus without missing confounder values to make sure missing completely at random assumption is not violated for our complete case analysis (Table S2).

2.2 | Existing large-scale blood pressure GWAS summary data

To strengthen the IV selection step and validate our causal finding, we also collected the existing large-scale GWAS summary data on BP from the meta-analysis of over 750,000 participants of European ancestry recruited from a total of 78 different cohorts (mainly from UKB and International Consortium of Blood Pressure (ICBP)) (Evangelou et al., 2018). We downloaded this large meta-analyzed GWAS summary statistics for SBP [https://gwas.mrcieu.ac.uk/datasets/ieu-b-38/, accessed on June 13, 2022] and DBP [https://gwas.mrcieu.ac.uk/datasets/ieu-b-39/, accessed on June 13, 2022] from IEU OpenGWAS project (Lyon et al., 2021). We used this existing meta-analyzed GWAS summary data to select IVs and conduct MR analysis as a validation of our causal findings using UKB alone (Figure 1, right).

2.3 | Mendelian randomization analyses

In this study, we performed a two-sample MR analysis to evaluate potential causal effects of SBP and DBP on FA of 39 WM tracts (Figure 1). We considered genetic variants as IVs, BP as the exposure, and FA as the outcome. In the GEset, we restricted to individuals with both genotype and BP data but no regional WM FA data to investigate the genetic–exposure associations. In the GOset, we restricted to individuals with both genotype, BP and regional WM FA data to investigate the genetic–outcome associations. There were no shared individuals between these two sets of samples. The two-sample MR analysis consists of two main analytical steps: (1) Selecting valid IVs that satisfied the IV assumptions; and (2) evaluating the causal effects using the selected IVs. For step (1), we also used the existing meta-analyzed GWAS summary statistics to select IVs to validate the findings. In addition, we performed two more MR analyses by switching the exposure and the outcome to rule out the reverse causality. We describe these steps in more details in the following subsections.

2.3.1 | Instrumental variable selection and assumption checking

There are three standard assumptions for IV selection in MR analysis (Angrist et al., 1996):

(i) The IV is associated with the exposure;
(ii) the IV is independent of the confounding factors; and
(iii) the IV is independent of the outcome given the exposure (i.e., the IV does not exert horizontal pleiotropy).

We selected valid IVs based on the above assumptions. First (i), we performed GWAS analysis of BP traits under an additive genetic model adjusting for sex, age, BMI, genotyping chip type (i.e., UKBL/UKB chip) and top 10 principal components (PCs) of population admixture using PLINK (version 1.9, http://www.cog-genomics.org/plink/1.9/) (Chang et al., 2015). We adopted a conservative cutoff (e.g., GWAS *p*-value $<1\times10^{-6}$) to select potential IVs and performed linkage disequilibrium (LD) clumping with r^2 threshold of .5 within window of 1 Mb to remove redundant highly correlated variants using PLINK (version 1.9, http://www.cog-genomics.org/plink/1.9/) (Chang et al., 2015). This choice of r^2 threshold and window size follows from the recent studies (Chen et al., 2021; Hou et al., 2022; Karlsson Linnér et al., 2019) to balance between being too stringent (too small r^2, too wide window size, very few IVs selected) and too conservative (too large r^2, too narrow window size, too many IVs selected). We also performed a sensitivity analysis by using the other thresholds and results remain largely consistent, reflecting that our parameter setting can select fewer but more specific and sufficiently strong IVs to achieve a good detection power (Table S3). Next (ii), we eliminated IVs associated with potential confounders by performing association test between each IV and each potential confounder (FDR-adjusted *p*-value >.05). Lastly (iii), we performed conditional independence tests to exclude IVs with evidence of horizontal pleiotropy (FDR-adjusted *p*-value >.1). In addition to satisfying the standard IV assumptions, we also followed more recent guidance for IV selection from Burgess et al. (2019) to select IVs that more biologically relevant to the exposure by performing the following steps: We first functionally annotated the IVs using an open-access online portal FAVOR (Functional Annotation of Variants; https://favor.genohub.org/) (Zhou et al., 2023). We then confined to those IVs with a biological link to BP reported in all published human GWAS studies collected by the NIH National Human Genome Research Institute GWAS catalogue (Buniello et al., 2019) through querying their corresponding functional annotations. When using the existing meta-analyzed GWAS summary data with large sample size to select IVs, we adopted a more standard cutoff (GWAS *p*-value $<5\times10^{-8}$) and performed LD clumping with an r^2 threshold of .1 (Lawlor et al., 2019; Qi & Chatterjee, 2019).

2.3.2 | Generalized version of inverse-variance weighted method and other MR methods to evaluate causality

We first performed an association analysis of FA in each WM tract with BP traits and restricted our causal analysis only to FA in regional WM with significantly negative association with BP (Leritz et al., 2010; Suzuki et al., 2017; van Dijk et al., 2004). We then used the selected IVs to perform the two-sample MR analysis using gen-IVW method developed by Burgess et al. (2016). The gen-IVW

method generalized the inverse-variance weighted method in MR analysis by taking correlations among IVs into account (Burgess et al., 2016). If a negative causal effect of BP on any WM tract was detected, we further performed MR analyses using other robust MR methods such as outlier-robust method (e.g., Mendelian randomization pleiotropy residual sum and outlier (MR-PRESSO) test (Verbanck et al., 2018)) and consensus method (e.g., weighted-median approach (Bowden et al., 2016)) for consistent findings (see details in Supplementary Material). A leave-one-out approach (LOOA) (Corbin et al., 2016) (i.e., leave one IV out at a time and rerun gen-IVW) was also performed as a sensitivity analysis (see details in Supplementary Material).

2.3.3 | Two additional two-sample MR analyses for reverse causality

A paradoxical relationship between low BP and reduced volumes of WM has been reported in some previous studies (Foster-Dingley et al., 2015; Td et al., 2003), suggesting that brain WM integrity might also cause changes in BP. To exclude the possibility of reverse causality, we preformed two additional two-sample MR analyses (i.e., MR reverse I and II) treating FA as the exposure and BP as the outcome. Due to the high correlation among human WM tracts treated as multiple exposures (Telford et al., 2017), we first estimated a general factor of FA (gFA) using factor analysis implemented in an R package "pysch" (version 1.7.8) (Revelle & Revelle, 2017) (see Figure S1). Then, we performed GWAS analysis on gFA adjusting for age, sex, BMI, genotyping chip type (i.e., UKBL/UKB chip), and top 10 PCs of population admixture by using PLINK (version 1.9, http://www.cog-genomics.org/plink/1.9/) (Chang et al., 2015).

In MR reverse I, following the scheme of bidirectional two-sample MR analysis (Zheng et al., 2017), we selected IVs according to IV assumptions (i)–(iii) with the switched exposure and outcome. In MR reverse II, we selected IVs that had significant association with both BP and gFA. Our MR reverse II was beyond the scope of bidirectional two-sample MR analysis, adding stronger evidence of whether the reverse causality existed.

All statistical analyses were conducted using R (version 4.0.5) (R Core Team, 2013). The gen-IVW, weighted-median approach and LOOA were implemented by using the R packages "*MendelianRandomization*" (version 0.5.1) (Yavorska & Burgess, 2017). The MR-PRESSO test was implemented by using the R package "*MR-PRESSO*" (version 0.1.0) (Verbanck et al., 2018). For both association and MR analyses, we controlled false discovery rate (FDR) at 5% to adjust for multiplicity using the Benjamini–Hochberg procedure (Benjamini & Hochberg, 1995).

3 | RESULTS

The GEset includes a total of 203,111 individuals to investigate the genetic–exposure associations, while the GOset includes 16,156 individuals to investigate the genetic–outcome associations. Baseline characteristics of individuals from the two sample sets are summarized in Table 1. The GEset consists of 91,792 males and 111,319 females, with mean age of 56.71 ($SD = 8.02$) years. The GOset consists of 7402 males and 8754 females, with mean age of 54.61 ($SD = 7.37$) years. There are a few self-reported diseases (Table S4) that may or may not confound our findings ((non-)insulin-dependent diabetes mellitus, hypertensive heart disease and chronic ischemic heart disease, etc.), we decide to include these individuals to ensure we have sufficient sample size for GWAS and MR analysis. But at the same time, we also perform sensitivity analysis to ensure our results are consistent while including versus excluding these subjects.

Based on the GWAS results from UKB cohort, we identified 8685 and 10,281 genetic variants associated with SBP and DBP (p-value $<1\times10^{-6}$). We further obtained 458 and 527 weakly correlated genetic variants by applying LD clumping for SBP and DBP, respectively. We then checked IV assumptions (ii) and (iii) to refine the pool of candidate IVs (see the number of candidate IVs passing each step for each FA measure in Table S5). A majority of these variants were mapped to BP-related genes (e.g., *CACNB2*, *MECOM*, *ADRB1*, and *ARHGAP42*) that have been reported in previous studies (Ehret & Caulfield, 2013; Fjorder et al., 2019; Levy et al., 2009; Tikhonoff et al., 2008) (full gene annotations summarized in Table S6). Likewise, IVs selected from the existing meta-analyzed GWAS summary data were also annotated to similar BP-related genes, which validated our IV selection step.

From the association analysis, we identified 37 and 36 WM tracts significantly negatively associated with SBP and DBP, respectively (Table S7; FDR-adjusted $p < .05$) and our MR analysis were restricted to only these tracts. The MR analyses further identified significantly negative causal effects of BP on 21 and 18 WM tracts for SBP and DBP, respectively (Table S7; FDR-adjusted $p < .05$). Figure 2 displays their standardized causal effect estimates (standardized coefficient ranging from −5.83 to −2.18; every 10 mmHg increase in BP leads to a decrease in FA value by .4%~2%, see more details in Table S7) from gen-IVW using IVs selected from UKB alone or existing meta-analyzed GWAS summary data. Higher BP caused a reduction in FA values of multiple WM tracts and such negative causal effects were consistent for both SBP and DBP, using IVs selected from UKB GWAS or existing meta-analyzed GWAS. We then applied alternative MR methods including MR-PRESSO (Verbanck et al., 2018) and weighted-median approach (Bowden et al., 2016) and identified 13 and 14 WM tracts (p-value <.05, Figure 3a) with consistently negative causal effects in all methods for SBP and DBP (standardized coefficient ranging from −5.05 to −2.58; every 10 mmHg increase in BP leads to a decrease in FA value by .4%~2%, see more details in Table S8), respectively. The LOOA also showed consistent causal effects on these WM tracts (see Supplementary File). To account for the effects of antihypertensive treatments, we also conducted a sensitivity analysis by including individuals who took antihypertensive treatments and detected similar results (see Table S8).

Figure 3b shows the location of a union set of 17 WM tracts adversely impacted by SBP or DBP in the brain (Rorden & Brett, 2000).

TABLE 1 Baseline characteristics of UK Biobank (UKB)'s individuals from the two sample sets used for two-sample Mendelian randomization (MR) analysis.

Characteristics	Whole sample set	Male	Female
Genetic–exposure association set (GEset)			
Number of individuals	203,111	91,792	111,319
Age, mean (*SD*)	56.71 (8.02)	56.8 (8.18)	56.63 (7.89)
BMI, mean (*SD*)	27.23 (4.65)	27.64 (4.12)	26.89 (5.02)
Smoking status (%)			
Never	111,836 (55.06%)	45,550 (49.62%)	66,286 (59.55%)
Previous	70,775 (34.85%)	35,260 (38.41%)	35,515 (31.9%)
Current	20,500 (10.09%)	10,982 (11.96%)	9518 (8.55%)
SBP, mmHg; mean (*SD*)	139.93 (19.63)	142.93 (18.46)	137.45 (20.21)
DBP, mmHg; mean (*SD*)	82.23 (10.64)	84.15 (10.51)	80.65 (10.49)
PP, mmHg; mean (*SD*)	57.70 (14.77)	58.79 (13.83)	56.8 (15.45)
Alcohol drinker status (%)			
Never	6037 (2.97%)	1477 (1.61%)	4560 (4.1%)
Previous	6826 (3.36%)	2894 (3.15%)	3932 (3.53%)
Current	190,248 (93.67%)	87,421 (95.24%)	102,827 (92.37%)
Fruit consumption, pieces/day; mean (*SD*)	2.99 (2.48)	2.67 (2.52)	3.25 (2.42)
Vegetable consumption, tablespoons/day; mean (*SD*)	4.81 (3.08)	4.57 (3.17)	5.01 (3.00)
Sedentary lifestyle, hours/day; mean (*SD*)	4.53 (2.48)	5.05 (2.69)	4.1 (2.19)
Insulin-dependent diabetes mellitus (self-reported) (%)	33 (.02%)	17 (.02%)	16 (.01%)
Non-insulin-dependent diabetes mellitus (self-reported) (%)	305 (.15%)	194 (.21%)	111 (.1%)
Hypertensive heart disease (self-reported) (%)	0 (0%)	0 (0%)	0 (0%)
Chronic ischemic heart disease (self-reported) (%)	0 (0%)	0 (0%)	0 (0%)
Genetic–outcome association set (GOset)			
Number of individuals	16,156	7402	8754
Age, mean (*SD*)	54.61 (7.37)	55.27 (7.54)	54.06 (7.18)
BMI, mean (*SD*)	26.28 (4.07)	26.77 (3.59)	25.86 (4.39)
Smoking status (%)			
Never	10,155 (62.86%)	4455 (60.19%)	5700 (65.11%)
Previous	5095 (31.54%)	2458 (33.21%)	2637 (30.12%)
Current	906 (5.61%)	489 (6.61%)	417 (4.76%)
SBP, mm Hg; mean (*SD*)	135.27 (17.97)	139.17 (16.73)	131.98 (18.33)
DBP, mm Hg; mean (*SD*)	80.61 (10.16)	82.75 (9.9)	78.8 (10.02)
PP, mm Hg; mean (*SD*)	54.66 (13.07)	56.42 (12.31)	53.18 (13.5)
Alcohol drinker status (%)			
Never	322 (1.99%)	97 (1.31%)	225 (2.57%)
Previous	302 (1.87%)	119 (1.61%)	183 (2.09%)
Current	15,532 (96.14%)	7186 (97.08%)	8346 (95.34%)
Fruit consumption, pieces/day; mean (*SD*)	3.07 (2.35)	2.8 (2.34)	3.3 (2.33)
Vegetable consumption, tablespoons/day; mean (*SD*)	4.74 (2.85)	4.52 (2.8)	4.92 (2.88)
Sedentary lifestyle, hours/day; mean (*SD*)	4.26 (2.35)	4.75 (2.54)	3.85 (2.09)
Insulin-dependent diabetes mellitus (self-reported) (%)	13 (.01%)	5 (.01%)	8 (.01%)
Non-insulin-dependent diabetes mellitus (self-reported) (%)	118 (.06%)	84 (.09%)	34 (.03%)
Hypertensive heart disease (self-reported) (%)	0 (0%)	0 (0%)	0 (0%)
Chronic ischemic heart disease (self-reported) (%)	0 (0%)	0 (0%)	0 (0%)

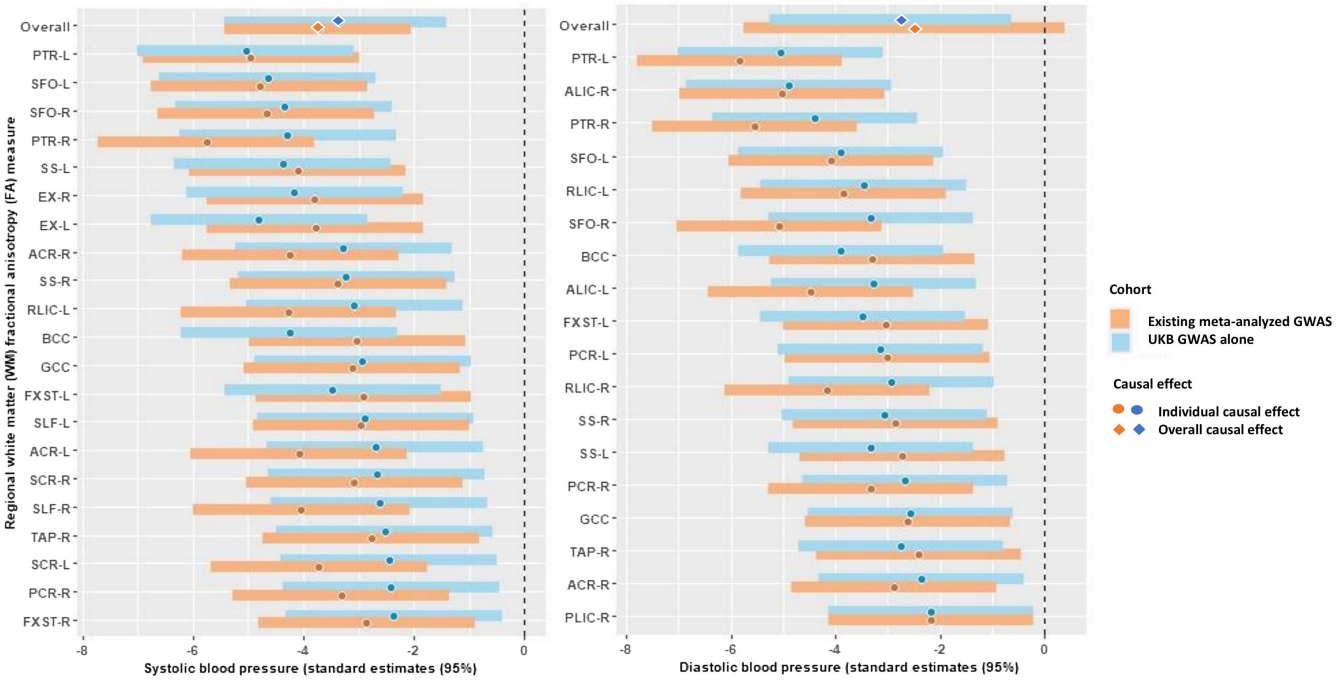

FIGURE 2 Forest plot to display the standardized causal effects of BP on WM FA tracts (21 and 18 with FDR-adjusted $p<.05$ for SBP (left) and DBP (right), respectively) using gen-IVW method and IVs selected from UKB GWAS alone (blue solid dots) or existing meta-analyzed GWAS summary (orange solid dots). The pooled effect sizes were obtained by a fixed effect model and represented by solid diamonds with blue and orange color, respectively. The 95% confidence interval (CI) was shown as bands. Y-axis refers to regional WM FA tracts, including bilateral posterior thalamic radiation (PTR-L/PTR-R), bilateral anterior limb of internal capsule (ALIC-L/ALIC-R), bilateral superior fronto-occipital fasciculus (SFO-L/SFO-R), bilateral sagittal stratum (SS-L/SS-R), bilateral external capsule (EX-L/EX-R), bilateral anterior corona radiata (ACR-L/ACR-R), bilateral retrolenticular part of internal capsule (RLIC-L/RLIC-R), body and genu of corpus callosum (BCC/GCC), bilateral Fornix (cres)/stria terminalis (FXST-L/FXST-R), bilateral superior longitudinal fasciculus (SLF-L/SLF-R), bilateral superior corona radiata (SCR-L/SCR-R), bilateral posterior corona radiata (PCR-L/PCR-R), right hemisphere of tapetum (TAP-R), and right hemisphere of posterior limb of internal capsule (PLIC-R).

The color represents -ln(p-value) generated from a meta-analysis of gen-IVW results from two BP traits and IVs selected from two GWAS results using adaptive-weighted Fisher's method (Huo et al., 2020) accounting for the possible heterogeneity across different BP traits and cohorts (Table S9). This includes bilateral PTR, bilateral SFO, bilateral ALIC, bilateral RLIC, bilateral SS, bilateral EX, BCC, GCC, FX/ST-L, PCR-L, and SCR-R. These brain regions are mainly related to the aspects of cognitive function (Di Carlo et al., 2019; Safadi et al., 2018; Schneider et al., 2021), motor ability (Hyett et al., 2018; Takeuchi & Kawashima, 2022), and memory (Bendlin et al., 2010; Maillard et al., 2012; Rizvi et al., 2020). Bilateral PTR and SFO were among the brain regions most adversely impacted by elevation of both BP traits (with most significant p-values), while bilateral EX was more sensitive to the change in SBP compared to that in DBP (Table S9).

We also performed two additional two-sample MR analyses by switching exposure and outcome. In MR reverse I where gFA was treated as the exposure and BP as the outcome, we selected 27 valid IVs for SBP and DBP, respectively (Table S10). Using these IVs, we did not observe significant causal effects of gFA on any BP (FDR-adjusted $p<.05$). In MR reverse II, none of variant was associated with both gFA and BP (Table S10). The results of these two additional MR analyses ruled out the reverse causality of gFA and BP, posing strong supports to our hypothesized causal pathway of BP on regional WM integrity.

4 | DISCUSSION

In this study, we integrated neuroimaging, genetics, and BP to conduct a two-sample MR analysis for evaluating the causal effects of BP on regional WM integrity measured by FA. We primarily conducted GWAS analysis on BP traits (i.e., SBP and DBP) and checked MR analysis assumptions using data from UKB cohort to select valid IVs for our two-sample MR analysis. The rigorous IV selection were further validated by existing large-scale GWAS summary data on BP (Evangelou et al., 2018). Most selected IVs were located in genes related to BP, functioning in intervention of heart rate via basal and agonist-stimulated receptor response (Johnson et al., 2011) and modulation of vascular resistance through calcium signals (Bai et al., 2017; Simonyte et al., 2018). Using these IVs, we applied the gen-IVW and other MR methods, and observed negative causal effects of BP traits on a union set of 17 WM tracts, including brain regions related to cognitive function, motor ability and memory, revealing that brain has differential vulnerability of WM deterioration to BP. These findings were consistent with the previous study

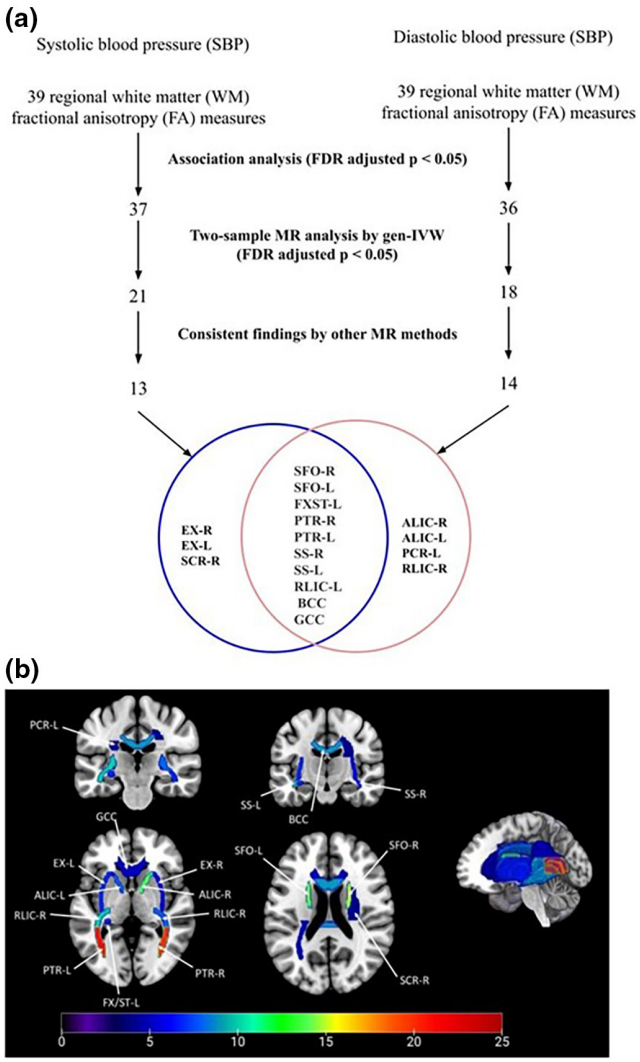

FIGURE 3 (a) The number of WM tracts identified for SBP and DBP at each step of analysis and a Venn diagram showing the union set of 17 regional WM FA tracts adversely impacted by SBP or DBP. (b) Location of the union set of 17 WM tracts in the brain. The color represents -ln(*p*-value) generated from a meta-analysis of gen-IVW results from two BP traits and IVs selected from two GWAS results using adaptive-weighted Fisher's method.

by considering the higher BP leads to WM abnormalities (Suzuki et al., 2017; Taylor-Bateman et al., 2022). Moreover, we identified specific WM tracts highly sensitive to changes in particular BP trait (e.g., bilateral EX more sensitive to SBP), which are worth of further explorations. The possible reverse causality was also carefully evaluated and eliminated to disentangle the causality link between BP and WM.

We found that 10 mmHg increases in BP can lead to a decrease in the FA values by .4%~2%, suggesting that the vascular health influences WM structure. The WM regions of SFO and PTR have been identified as being causally affected by high BP because the fibers within these regions are related to memory and cognitive functions with a relatively high risk of brain atrophy. The SBP-specific causal effect on bilateral EX was consistent with the findings in the previous studies (Acosta et al., 2022; Taschler et al., 2022). The DBP-specific causal effect on bilateral ALIC, RLIC-R, and PCR-L has also been reported in the previous literature (Hyett et al., 2018; Takeuchi & Kawashima, 2022), which is supportive of causal relationships between increasing DBP and the development of psychomotor dysfunctions. The present findings demonstrate the regional-specific neural implications of elevated BP on brain structure, which could possibly aid in the prevention of white matter loss in the future.

Genetic variants selected as IVs in the study mainly resided in genes *CACNB2* and *ARHGAP42* and were shared in both BP traits. Their encoded proteins have been identified to be essential to intracellular calcium homeostasis by modulating calcium channel activity (Foster-Dingley et al., 2015) and limiting contractility of vascular smooth muscle cells to exert its protective function (Bai et al., 2017), respectively. Mutations occurred within these two genes will damage calcium buffering capacities and malfunction calcium channel activities, resulting in neuronal autophagy and neurodegenerative diseases such as Alzheimer's disease and Parkinson's disease (Zündorf & Reiser, 2011). Most of these variants were located in intronic regions of the genes, and further studies need to be conducted to understand the biology behind these genes in regulating BP which in turn alters white matter microstructure in the brain, by integrating with various other omics data such as epigenomic profiles and incorporating expression quantitative trait locus (QTL) database.

This study has several strengths. The two-sample MR study is a powerful method to make causal inferences of modifiable exposure on the outcome in observational studies by using genetic variants as IVs. We applied it to two large cohorts (primarily UKB cohort, and then large existing meta-analyzed GWAS cohort as validation) with high-quality data, providing a greater statistical power to better understand the causal relationship between BP with regional WM FA diminishing confounding and reverse causality. We also restricted our study population to European ancestry to minimize the confounding raising from population stratification. Additionally, we excluded individuals taking antihypertensive treatments and having extreme values of WMH to eliminate the neuroprotective effects of antihypertensive treatments and bias effects of total volume of WMH on brain structures and functions, leading to unbiased causal effects of genetically determined BP across brain regions. We conducted various sensitivity analyses and used several robust MR methods to test the validity and consistency of our causal findings. For example, MR-PRESSO (Verbanck et al., 2018) was adopted to evaluate pleiotropy bias, weighted-median approach (Bowden et al., 2016) to assess invalid instrument bias of IVs and LOOA (Corbin et al., 2016) to test the sensitivity of single IV, the results of which were consistent with our primary gen-IVW results, indicating the reliability of our causal findings.

However, this study has some limitations with potential extensions. First, although we avoided the confounding effects of antihypertensive treatments by removing the participants taking this treatment, further study is encouraged to account for the effects of antihypertensive medication. Also, the UKB cohort has a healthy

volunteer selection bias (Fry et al., 2017), it is critical to validate the generalizability of our results using populations with a wider range of socioeconomic profiles, instead of restricted to the European ancestry. Second, in this study, we investigated the causal effect of BP on multiple correlated outcomes (i.e., FA tracts in different brain regions). The multivariate MR analysis enables assessing multiple correlated exposures simultaneously (Burgess & Thompson, 2015; Sanderson et al., 2019) through including genetic variants from each risk factor into the same model (Davies et al., 2019). From this perspective, current MR analysis can be extended to multivariable MR method, when other CVD risk factors (e.g., cholesterol, alcohol drink and etc.) other than BP are of major interest in future studies. Additionally, age and BP level stratification would be worth incorporating into our MR analysis as suggested in the previous study (Lane et al., 2019). However, since the sample size after stratification is small weakening the power of the GWAS and MR analyses and the UKB cohort covers a relatively narrow age range (40~69) with little heterogeneity, we will leave stratified analysis to new cohort in future studies. Third, the sensitivity analyses by MR methods can be further improved. For example, MR-PRESSO (Verbanck et al., 2018) detected and corrected causal effects in the presence of horizontal pleiotropic outliers, but the causal effects were only detectable when at least 50% of the variants were valid instruments and satisfied the Instrument Strength Independent of Direct Effect (InSIDE) condition (Bowden et al., 2015).

High BP is a common risk factor for the development of CVD with progressive hypertension, which greatly damages the WM integrity in the brain. Our results demonstrated strong evidences for the causal role of genetically determined BP in WM degradation of different parts of brain. These findings are critical to our understanding of the relationship between CVD risk factors and regional brain structural change and can be used for prevention of WM loss in the future.

DECLARATION OF TRANSPARENCY

The authors, reviewers and editors affirm that in accordance to the policies set by the *Journal of Neuroscience Research*, this manuscript presents an accurate and transparent account of the study being reported and that all critical details describing the methods and results are present.

AUTHOR CONTRIBUTIONS

Zhenyao Ye: Data curation, Formal analysis, Writing - Original draft preparation. Chen Mo: Data curation, Formal analysis, Writing - Original draft preparation. Song Liu: Data curation, Writing - Reviewing and Editing. Si Gao: Writing - Reviewing and Editing. Li Feng: Writing - Reviewing and Editing. Boao Zhao: Writing - Reviewing and Editing. Travis Canida: Writing - Reviewing and Editing. Yu-Chia Wu: Writing - Reviewing and Editing. Kathryn S Hatch: Writing - Reviewing and Editing. Yizhou Ma: Writing - Reviewing and Editing. Braxton D. Mitchell: Writing - Reviewing and Editing. L.Elliot Hong: Writing - Reviewing and Editing. Peter Kochunov: Writing - Reviewing and Editing, Funding acquisition. Chixiang Chen: Writing - Reviewing and Editing. Bingxin Zhao: Writing - Reviewing and Editing. Tianzhou Ma: Supervision, Writing - Reviewing and Editing, Funding acquisition. Shuo Chen: Supervision, Writing - Reviewing and Editing, Funding acquisition.

ACKNOWLEDGMENTS

This work was supported by the National Institute on Drug Abuse (NIDA) of National Institutes of Health under award number 1DP1DA048968-01, University of Maryland Grand Challenge grant, University of Maryland MPower Brain Health and Human Performance seed grant, and the National Institutes of Health under award numbers R01MH123163, R01EB015611, and S10OD023696.

FUNDING INFORMATION

Research reported in this publication was supported by the National Institute on Drug Abuse (NIDA) of National Institutes of Health under award number 1DP1DA048968-01 to ZY, CM, SC, and TM, University of Maryland Grand Challenge grant, University of Maryland MPower Brain Health and Human Performance seed grant to PK, SC, and TM, and the National Institutes of Health under award numbers R01MH123163, R01EB015611, and S10OD023696 to PK.

CONFLICT OF INTEREST STATEMENT

The authors report no conflict of interest.

PEER REVIEW

The peer review history for this article is available at https://www.webofscience.com/api/gateway/wos/peer-review/10.1002/jnr.25205.

DATA AVAILABILITY STATEMENT

The raw genetic and phenotypic data used in the current study are available from the UK Biobank (UKB), which can be accessed via https://www.ukbiobank.ac.uk/.

ORCID

Zhenyao Ye https://orcid.org/0000-0002-6530-1088
Si Gao https://orcid.org/0000-0002-4473-1142
Tianzhou Ma https://orcid.org/0000-0003-3605-0811

REFERENCES

Acosta, J., Haider, S. P., Rivier, C., Leasure, A. C., Sheth, K. N., Falcone, G. J., & Payabvash, S. (2022). Pervasive white matter microstructure dysintegrity related to high blood pressure among asymptomatic population. *Stroke*, *53*, A9.

Alfaro-Almagro, F., Jenkinson, M., Bangerter, N. K., Andersson, J. L., Griffanti, L., Douaud, G., Sotiropoulos, S. N., Jbabdi, S., Hernandez-Fernandez, M., & Vallee, E. (2018). Image processing and quality control for the first 10,000 brain imaging datasets from UK Biobank. *NeuroImage*, *166*, 400–424.

Allen, B., Muldoon, M. F., Gianaros, P. J., & Jennings, J. R. (2016). Higher blood pressure partially links greater adiposity to reduced brain white matter integrity. *American Journal of Hypertension*, *29*, 1029–1037.

Angrist, J. D., Imbens, G. W., & Rubin, D. B. (1996). Identification of causal effects using instrumental variables. *Journal of the American Statistical Association*, *91*, 444–455.

Bai, X., Mangum, K. D., Dee, R. A., Stouffer, G. A., Lee, C. R., Oni-Orisan, A., Patterson, C., Schisler, J. C., Viera, A. J., & Taylor, J. M. (2017). Blood pressure–associated polymorphism controls ARHGAP42 expression via serum response factor DNA binding. *The Journal of Clinical Investigation*, *127*, 670–680.

Bendlin, B. B., Fitzgerald, M. E., Ries, M. L., Xu, G., Kastman, E. K., Thiel, B. W., Rowley, H. A., Lazar, M., Alexander, A. L., & Johnson, S. C. (2010). White matter in aging and cognition: A cross-sectional study of microstructure in adults aged eighteen to eighty-three. *Developmental Neuropsychology*, *35*, 257–277.

Benjamini, Y., & Hochberg, Y. (1995). Controlling the false discovery rate: A practical and powerful approach to multiple testing. *Journal of the Royal Statistical Society: Series B: Methodological*, *57*, 289–300.

Bowden, J., Davey Smith, G., & Burgess, S. (2015). Mendelian randomization with invalid instruments: Effect estimation and bias detection through Egger regression. *International Journal of Epidemiology*, *44*, 512–525.

Bowden, J., Davey Smith, G., Haycock, P. C., & Burgess, S. (2016). Consistent estimation in Mendelian randomization with some invalid instruments using a weighted median estimator. *Genetic Epidemiology*, *40*, 304–314.

Buniello, A., MacArthur, J. A. L., Cerezo, M., Harris, L. W., Hayhurst, J., Malangone, C., McMahon, A., Morales, J., Mountjoy, E., & Sollis, E. (2019). The NHGRI-EBI GWAS Catalog of published genome-wide association studies, targeted arrays and summary statistics 2019. *Nucleic Acids Research*, *47*, D1005–D1012.

Burgess, S., Dudbridge, F., & Thompson, S. G. (2016). Combining information on multiple instrumental variables in Mendelian randomization: Comparison of allele score and summarized data methods. *Statistics in Medicine*, *35*, 1880–1906.

Burgess, S., Smith, G. D., Davies, N. M., Dudbridge, F., Gill, D., Glymour, M. M., Hartwig, F. P., Holmes, M. V., Minelli, C., & Relton, C. L. (2019). Guidelines for performing Mendelian randomization investigations. *Wellcome Open Research*, *4*, 186. https://doi.org/10.12688/wellcomeopenres.15555.2

Burgess, S., & Thompson, S. G. (2015). Multivariable Mendelian randomization: The use of pleiotropic genetic variants to estimate causal effects. *American Journal of Epidemiology*, *181*, 251–260.

Bycroft, C., Freeman, C., Petkova, D., Band, G., Elliott, L. T., Sharp, K., Motyer, A., Vukcevic, D., Delaneau, O., & O'Connell, J. (2017). Genome-wide genetic data on ~500,000 UK Biobank participants. BioRxiv:166298.

Chang, C. C., Chow, C. C., Tellier, L. C., Vattikuti, S., Purcell, S. M., & Lee, J. J. (2015). Second-generation PLINK: Rising to the challenge of larger and richer datasets. *GigaScience*, *4*, 7. https://doi.org/10.1186/s13742-015-0047-8

Chen, G., Wang, Q., Xue, R., Liu, X., & Yu, H. (2021). Examining the causal inference of leptin and soluble plasma leptin receptor levels on schizophrenia: A Mendelian randomization study. *Frontiers in Psychiatry*, *12*, 753224.

Chobanian, A. V., Bakris, G. L., Black, H. R., Cushman, W. C., Green, L. A., Izzo, J. L., Jr., Jones, D. W., Materson, B. J., Oparil, S., & Wright, J. T., Jr. (2003). Seventh report of the joint national committee on prevention, detection, evaluation, and treatment of high blood pressure. *Hypertension*, *42*, 1206–1252.

Conroy, M., Sellors, J., Effingham, M., Littlejohns, T. J., Boultwood, C., Gillions, L., Sudlow, C., Collins, R., & Allen, N. E. (2019). The advantages of UK Biobank's open-access strategy for health research. *Journal of Internal Medicine*, *286*, 389–397.

Corbin, L. J., Richmond, R. C., Wade, K. H., Burgess, S., Bowden, J., Smith, G. D., & Timpson, N. J. (2016). BMI as a modifiable risk factor for type 2 diabetes: Refining and understanding causal estimates using Mendelian randomization. *Diabetes*, *65*, 3002–3007.

Davies, N. M., Hill, W. D., Anderson, E. L., Sanderson, E., Deary, I. J., & Davey Smith, G. (2019). Multivariable two-sample Mendelian randomization estimates of the effects of intelligence and education on health. *eLife*, *8*, e43990.

Di Carlo, D. T., Benedetto, N., Duffau, H., Cagnazzo, F., Weiss, A., Castagna, M., Cosottini, M., & Perrini, P. (2019). Microsurgical anatomy of the sagittal stratum. *Acta Neurochirurgica*, *161*, 2319–2327.

Ehret, G. B., & Caulfield, M. J. (2013). Genes for blood pressure: An opportunity to understand hypertension. *European Heart Journal*, *34*, 951–961.

Evangelou, E., Warren, H. R., Mosen-Ansorena, D., Mifsud, B., Pazoki, R., Gao, H., Ntritsos, G., Dimou, N., Cabrera, C. P., & Karaman, I. (2018). Genetic analysis of over 1 million people identifies 535 new loci associated with blood pressure traits. *Nature Genetics*, *50*, 1412–1425.

Fjorder, A. S., Rasmussen, M. B., Mehrjouy, M. M., Nazaryan-Petersen, L., Hansen, C., Bak, M., Grarup, N., Nørremølle, A., Larsen, L. A., & Vestergaard, H. (2019). Haploinsufficiency of ARHGAP42 is associated with hypertension. *European Journal of Human Genetics*, *27*, 1296–1303.

Foster-Dingley, J. C., van der Grond, J., Moonen, J. E., van den Berg-Huijsmans, A. A., de Ruijter, W., van Buchem, M. A., de Craen, A. J., & van der Mast, R. C. (2015). Lower blood pressure is associated with smaller subcortical brain volumes in older persons. *American Journal of Hypertension*, *28*, 1127–1133.

Fry, A., Littlejohns, T. J., Sudlow, C., Doherty, N., Adamska, L., Sprosen, T., Collins, R., & Allen, N. E. (2017). Comparison of sociodemographic and health-related characteristics of UK Biobank participants with those of the general population. *American Journal of Epidemiology*, *186*, 1026–1034.

Fuchs, F. D., & Whelton, P. K. (2020). High blood pressure and cardiovascular disease. *Hypertension*, *75*, 285–292.

Georgakis, M. K., Gill, D., Webb, A. J., Evangelou, E., Elliott, P., Sudlow, C. L., Dehghan, A., Malik, R., Tzoulaki, I., & Dichgans, M. (2020). Genetically determined blood pressure, antihypertensive drug classes, and risk of stroke subtypes. *Neurology*, *95*, e353–e361.

Gons, R. A., de Laat, K. F., van Norden, A. G., van Oudheusden, L. J., van Uden, I. W., Norris, D. G., Zwiers, M. P., & de Leeuw, F.-E. (2010). Hypertension and cerebral diffusion tensor imaging in small vessel disease. *Stroke*, *41*, 2801–2806.

Hou, L., Yu, Y., Sun, X., Liu, X., Yu, Y., Li, H., & Xue, F. (2022). Causal mediation analysis with multiple causally non-ordered and ordered mediators based on summarized genetic data. *Statistical Methods in Medical Research*, *31*, 1263–1279.

Huo, Z., Tang, S., Park, Y., & Tseng, G. (2020). P-value evaluation, variability index and biomarker categorization for adaptively weighted Fisher's meta-analysis method in omics applications. *Bioinformatics*, *36*, 524–532.

Hyett, M. P., Perry, A., Breakspear, M., Wen, W., & Parker, G. B. (2018). White matter alterations in the internal capsule and psychomotor impairment in melancholic depression. *PLoS One*, *13*, e0195672.

Johnson, A. D., Newton-Cheh, C., Chasman, D. I., Ehret, G. B., Johnson, T., Rose, L., Rice, K., Verwoert, G. C., Launer, L. J., & Gudnason, V. (2011). Association of hypertension drug target genes with blood pressure and hypertension in 86 588 individuals. *Hypertension*, *57*, 903–910.

Jones, D. K., Lythgoe, D., Horsfield, M. A., Simmons, A., Williams, S. C., & Markus, H. S. (1999). Characterization of white matter damage in ischemic leukoaraiosis with diffusion tensor MRI. *Stroke*, *30*, 393–397.

Karlsson Linnér, R., Biroli, P., Kong, E., Meddens, S. F. W., Wedow, R., Fontana, M. A., Lebreton, M., Tino, S. P., Abdellaoui, A.,

Hammerschlag, A. R., Nivard, M. G., Okbay, A., Rietveld, C. A., Timshel, P. N., Trzaskowski, M., De Vlaming, R., Zünd, C. L., Bao, Y., Buzdugan, L., … Beauchamp, J. P. (2019). Genome-wide association analyses of risk tolerance and risky behaviors in over 1 million individuals identify hundreds of loci and shared genetic influences. *Nature Genetics*, *51*(2), 245–257.

Lane, C. A., Barnes, J., Nicholas, J. M., Sudre, C. H., Cash, D. M., Parker, T. D., Malone, I. B., Lu, K., James, S. N., Keshavan, A., Murray-Smith, H., Wong, A., Buchanan, S. M., Keuss, S. E., Gordon, E., Coath, W., Barnes, A., Dickson, J., Modat, M., … Schott, J. M. (2019). Associations between blood pressure across adulthood and late-life brain structure and pathology in the neuroscience substudy of the 1946 British birth cohort (Insight 46): An epidemiological study. *Lancet Neurology*, *18*, 942–952.

Lawlor, D. A., Harbord, R. M., Sterne, J. A., Timpson, N., & Davey Smith, G. (2008). Mendelian randomization: Using genes as instruments for making causal inferences in epidemiology. *Statistics in Medicine*, *27*, 1133–1163.

Lawlor, D. A., Wade, K., Borges, M. C., Palmer, T., Hartwig, F. P., Hemani, G., & Bowden, J. (2019). A Mendelian randomization dictionary: Useful definitions and descriptions for undertaking. *Understanding and Interpreting Mendelian Randomization Studies OSF Preprints*.

Leritz, E. C., Salat, D. H., Milberg, W. P., Williams, V. J., Chapman, C. E., Grande, L. J., Rudolph, J. L., Schnyer, D. M., Barber, C. E., & Lipsitz, L. A. (2010). Variation in blood pressure is associated with white matter microstructure but not cognition in African Americans. *Neuropsychology*, *24*, 199–208.

Levy, D., Ehret, G. B., Rice, K., Verwoert, G. C., Launer, L. J., Dehghan, A., Glazer, N. L., Morrison, A. C., Johnson, A. D., & Aspelund, T. (2009). Genome-wide association study of blood pressure and hypertension. *Nature Genetics*, *41*, 677–687.

Li, X., Salami, A., Avelar-Pereira, B., Bäckman, L., & Persson, J. (2022). White-matter integrity and working memory: Links to aging and dopamine-related genes. *eNeuro*, *9*, ENEURO.0413-21.2022.

Lyon, M. S., Andrews, S. J., Elsworth, B., Gaunt, T. R., Hemani, G., & Marcora, E. (2021). The variant call format provides efficient and robust storage of GWAS summary statistics. *Genome Biology*, *22*, 1–10.

Madden, D. J., Bennett, I. J., & Song, A. W. (2009). Cerebral white matter integrity and cognitive aging: Contributions from diffusion tensor imaging. *Neuropsychology Review*, *19*, 415–435.

Maillard, P., Seshadri, S., Beiser, A., Himali, J. J., Au, R., Fletcher, E., Carmichael, O., Wolf, P. A., & DeCarli, C. (2012). Effects of systolic blood pressure on white-matter integrity in young adults in the Framingham Heart Study: A cross-sectional study. *Lancet Neurology*, *11*, 1039–1047.

Malik, R., Georgakis, M. K., Vujkovic, M., Damrauer, S. M., Elliott, P., Karhunen, V., Giontella, A., Fava, C., Hellwege, J. N., & Shuey, M. M. (2021). Relationship between blood pressure and incident cardiovascular disease: Linear and nonlinear mendelian randomization analyses. *Hypertension*, *77*, 2004–2013.

Pazoki, R., Dehghan, A., Evangelou, E., Warren, H., Gao, H., Caulfield, M., Elliott, P., & Tzoulaki, I. (2018). Genetic predisposition to high blood pressure and lifestyle factors: Associations with midlife blood pressure levels and cardiovascular events. *Circulation*, *137*, 653–661.

Qi, G., & Chatterjee, N. (2019). Mendelian randomization analysis using mixture models for robust and efficient estimation of causal effects. *Nature Communications*, *10*, 1–10.

R Core Team. (2013). R: A language and environment for statistical computing.

Revelle, W., & Revelle, M. W. (2015). Package 'psych'. *The comprehensive R archive network* 337, 338.

Rizvi, B., Lao, P. J., Colón, J., Hale, C., Igwe, K. C., Narkhede, A., Budge, M., Manly, J. J., Schupf, N., & Brickman, A. M. (2020). Tract-defined regional white matter hyperintensities and memory. *NeuroImage: Clinical*, *25*, 102143.

Rorden, C., & Brett, M. (2000). Stereotaxic display of brain lesions. *Behavioural Neurology*, *12*, 191–200.

Safadi, Z., Grisot, G., Jbabdi, S., Behrens, T. E., Heilbronner, S. R., McLaughlin, N. C., Mandeville, J., Versace, A., Phillips, M. L., & Lehman, J. F. (2018). Functional segmentation of the anterior limb of the internal capsule: Linking white matter abnormalities to specific connections. *The Journal of Neuroscience*, *38*, 2106–2117.

Salat, D. H., Williams, V. J., Leritz, E. C., Schnyer, D. M., Rudolph, J. L., Lipsitz, L. A., McGlinchey, R. E., & Milberg, W. P. (2012). Interindividual variation in blood pressure is associated with regional white matter integrity in generally healthy older adults. *NeuroImage*, *59*, 181–192.

Sanderson, E., Davey Smith, G., Windmeijer, F., & Bowden, J. (2019). An examination of multivariable Mendelian randomization in the single-sample and two-sample summary data settings. *International Journal of Epidemiology*, *48*, 713–727.

Sargurupremraj, M., Suzuki, H., Jian, X., Sarnowski, C., Evans, T. E., Bis, J. C., Eiriksdottir, G., Sakaue, S., Terzikhan, N., & Habes, M. (2020). Cerebral small vessel disease genomics and its implications across the lifespan. *Nature Communications*, *11*, 1–18.

Schneider, R., Matusche, B., Genç, E., Gold, R., Bellenberg, B., & Lukas, C. (2021). Microstructural white matter alterations in cognitively impaired patients at early stages of multiple sclerosis. *Clinical Neuroradiology*, *31*, 993–1003.

Simonyte, S., Kuciene, R., Dulskiene, V., & Lesauskaite, V. (2018). Association between ATP2B1 and CACNB2 polymorphisms and high blood pressure in a population of Lithuanian children and adolescents: A cross-sectional study. *BMJ Open*, *8*, e019902.

Smith, S. M., Jenkinson, M., Johansen-Berg, H., Rueckert, D., Nichols, T. E., Mackay, C. E., Watkins, K. E., Ciccarelli, O., Cader, M. Z., & Matthews, P. M. (2006). Tract-based spatial statistics: Voxelwise analysis of multi-subject diffusion data. *NeuroImage*, *31*, 1487–1505.

Sudlow, C., Gallacher, J., Allen, N., Beral, V., Burton, P., Danesh, J., Downey, P., Elliott, P., Green, J., & Landray, M. (2015). UK biobank: An open access resource for identifying the causes of a wide range of complex diseases of middle and old age. *PLoS Medicine*, *12*, e1001779.

Suzuki, H., Gao, H., Bai, W., Evangelou, E., Glocker, B., O'Regan, D. P., Elliott, P., & Matthews, P. M. (2017). Abnormal brain white matter microstructure is associated with both pre-hypertension and hypertension. *PLoS One*, *12*, e0187600.

Takeuchi, H., & Kawashima, R. (2022). Effects of diastolic blood pressure on brain structures and cognitive functions in middle and old ages: Longitudinal analyses. *Nutrients*, *14*, 2464.

Taschler, B., Smith, S. M., & Nichols, T. E. (2022). Causal inference on neuroimaging data with Mendelian randomisation. *NeuroImage*, *258*, 119385.

Taylor-Bateman, V., Gill, D., Georgakis, M. K., Malik, R., Munroe, P., & Traylor, M. (2022). Cardiovascular risk factors and MRI markers of cerebral small vessel disease: A Mendelian randomization study. *Neurology*, *98*, e343–e351.

Td, H., Skoog, I., Oudkerk, M., de Leeuw, F.-E., de Groot, J. C., Hofman, A., & Breteler, M. (2003). Association between blood pressure levels over time and brain atrophy in the elderly. *Neurobiology of Aging*, *24*, 307–313.

Telford, E. J., Cox, S. R., Fletcher-Watson, S., Anblagan, D., Sparrow, S., Pataky, R., Quigley, A., Semple, S. I., Bastin, M. E., & Boardman, J. P. (2017). A latent measure explains substantial variance in white matter microstructure across the newborn human brain. *Brain Structure & Function*, *222*, 4023–4033.

Thompson, P. M., Stein, J. L., Medland, S. E., Hibar, D. P., Vasquez, A. A., Renteria, M. E., Toro, R., Jahanshad, N., Schumann, G., & Franke, B. (2014). The ENIGMA Consortium: Large-scale collaborative analyses of neuroimaging and genetic data. *Brain Imaging and Behavior*, *8*, 153–182.

Tikhonoff, V., Hasenkamp, S., Kuznetsova, T., Thijs, L., Jin, Y., Richart, T., Zhang, H., Brand-Herrmann, S., Brand, E., & Casiglia, E. (2008). Blood pressure and metabolic phenotypes in relation to the ADRB1 Arg389Gly and ADRA2B I/D polymorphisms in a White population. *Journal of Human Hypertension*, *22*, 864–867.

Tilaki, K. H. (2012). Methodological issues of confounding in analytical epidemiologic studies. *Caspian Journal of Internal Medicine*, *3*, 488.

Timpe, J., Rowe, K., Matsui, J., Magnotta, V., & Denburg, N. (2011). White matter integrity, as measured by diffusion tensor imaging, distinguishes between impaired and unimpaired older adult decision-makers: A preliminary investigation. *Journal of Cognitive Psychology*, *23*, 760–767.

UK Biobank. (2013). Repeat Assessment Data: September 2013. https://biobank.ctsu.ox.ac.uk/~bbdatan/Repeat_assessment_doc_v1.0.pdf

UK Biobank. (2014). Repeat assessment: Participant characteristics of responders vs. non-responders.

van Dijk, E. J., Breteler, M. M., Schmidt, R., Berger, K., Nilsson, L.-G., Oudkerk, M., Pajak, A., Sans, S., de Ridder, M., & Dufouil, C. (2004). The association between blood pressure, hypertension, and cerebral white matter lesions: Cardiovascular determinants of dementia study. *Hypertension*, *44*, 625–630.

Verbanck, M., Chen, C., Neale, B., & Do, R. (2018). Detection of widespread horizontal pleiotropy in causal relationships inferred from Mendelian randomization between complex traits and diseases. *Nature Genetics*, *50*, 693–698.

Walsh, M., Montojo, C. A., Sheu, Y.-S., Marchette, S. A., Harrison, D. M., Newsome, S. D., Zhou, F., Shelton, A. L., & Courtney, S. M. (2011). Object working memory performance depends on microstructure of the frontal-occipital fasciculus. *Brain Connectivity*, *1*, 317–329.

Williamson, W., Lewandowski, A. J., Forkert, N. D., Griffanti, L., Okell, T. W., Betts, J., Boardman, H., Siepmann, T., McKean, D., & Huckstep, O. (2018). Association of cardiovascular risk factors with MRI indices of cerebrovascular structure and function and white matter hyperintensities in young adults. *JAMA*, *320*, 665–673.

Yavorska, O. O., & Burgess, S. (2017). MendelianRandomization: An R package for performing Mendelian randomization analyses using summarized data. *International Journal of Epidemiology*, *46*, 1734–1739.

Zhao, B., Zhang, J., Ibrahim, J. G., Luo, T., Santelli, R. C., Li, Y., Li, T., Shan, Y., Zhu, Z., & Zhou, F. (2021). Large-scale GWAS reveals genetic architecture of brain white matter microstructure and genetic overlap with cognitive and mental health traits (n = 17,706). *Molecular Psychiatry*, *26*(8), 3943–3955.

Zheng, J., Baird, D., Borges, M.-C., Bowden, J., Hemani, G., Haycock, P., Evans, D. M., & Smith, G. D. (2017). Recent developments in Mendelian randomization studies. *Current Epidemiology Reports*, *4*, 330–345.

Zhou, H., Arapoglou, T., Li, X., Li, Z., Zheng, X., Moore, J., Asok, A., Kumar, S., Blue, E. E., & Buyske, S. (2023). FAVOR: Functional annotation of variants online resource and annotator for variation across the human genome. *Nucleic Acids Research*, *51*, D1300–D1311.

Zündorf, G., & Reiser, G. (2011). Calcium dysregulation and homeostasis of neural calcium in the molecular mechanisms of neurodegenerative diseases provide multiple targets for neuroprotection. *Antioxidants & Redox Signaling*, *14*, 1275–1288.

SUPPORTING INFORMATION

Additional supporting information can be found online in the Supporting Information section at the end of this article.

Figure S1. Factor analysis for a general factor of FA (gFA). Panel (a): a bar graph shows each FA measure's factor loadings in a separate facet. Panel (b): a scree plot of 4 factors determined by the factor analysis with a Tucker Lewis Index of factoring reliability at .657.

Figure S2. Histogram of normalized white matter hyperintensities (WMH) data provided in UK Biobank (UKB).

Data S1. Transparent Science Questionnaire for Authors

Table S1. A list of 39 regional white matter (WM) integrity measured by fractional antitropy (FA).

Table S2. Results of two-sample *t*-test for each confounder separately comparing the FA values of those with versus without missing confounder values (univariate version of little MCAR test).

Table S3. Numbers of candidate instrumental variables (IVs) determined at each step and numbers of significant causal effects detected implemented with our statistical method by separately using different LD clumping settings.

Table S4. Self-report neurological characteristics of UK Biobank's participants from two independent association sample sets for the two-sample Mendelian randomization (MR) analysis.

Table S5. Numbers of candidate instrumental variables (IVs) determined at each step of our statistical method by separately using UK Biobank (UKB) GWAS and existing meta-analyzed GWAS.

Table S6. Gene annotations for determined valid instrumental variables (IVs) carried into the two-sample Mendelian randomization (MR) analysis by separately using UK Biobank (UKB) GWAS and existing meta-analyzed GWAS.

Table S7. Results of association analysis and Mendelian randomization analysis (implemented with generalized version of inverse-variance weighted (gen-IVW) approach) in the study samples.

Table S8. Results of alternative Mendelian randomization (MR) approach and sensitivity analyses by using data from UK Biobank (UKB) cohort.

Table S9. Results of adaptively weighted (AW) Fisher's method and Mendelian randomization analysis implemented with a generalized version of inverse-variance weight method (gen-IVW).

Table S10. Results and numbers of candidate instrumental variables (IVs) in each step of our two reverse two-sample Mendelian randomization (MR) analyses using UK Biobank (UKB) cohort.

Data S2. Leave-one-out analysis for SBP with each FA and Leave-one-out analysis for DBP with each FA.

How to cite this article: Ye, Z., Mo, C., Liu, S., Gao, S., Feng, L., Zhao, B., Canida, T., Wu, Y.-C., Hatch, K. S., Ma, Y., Mitchell, B. D., Hong, L. E., Kochunov, P., Chen, C., Zhao, B., Chen, S., & Ma, T. (2023). Deciphering the causal relationship between blood pressure and regional white matter integrity: A two-sample Mendelian randomization study. *Journal of Neuroscience Research*, *101*, 1471–1483. https://doi.org/10.1002/jnr.25205